JOURNAL OF BACTERIOLOGY, Apr. 2005, p. 2416–2425 Vol. 187, No. 7
0021-9193/05/$08.00+0 doi:10.1128/JB.187.7.2416–2425.2005
Copyright © 2005, American Society for Microbiology. All Rights Reserved.

The Presumptive Magnetosome Protein Mms16 Is a Poly(3-Hydroxybutyrate) Granule-Bound Protein (Phasin) in *Magnetospirillum gryphiswaldense*

Daniel Schultheiss,[1] René Handrick,[2]† Dieter Jendrossek,[2]
Marianne Hanzlik,[3] and Dirk Schüler[1]*

Max Planck Institute for Marine Microbiology, Bremen,[1] Institute for Microbiology, University Stuttgart, Stuttgart,[2] and Institute for Technical Chemistry, Department of Electron Microscopy, Technical University Munich, Garching,[3] Germany

Received 19 August 2004/Accepted 20 December 2004

The Mms16 protein has been previously found to be associated with isolated magnetosomes from two *Magnetospirillum* strains. A function of this protein as a magnetosome-specific GTPase involved in the formation of intracellular magnetosome membrane vesicles was suggested (Y. Okamura, H. Takeyama, and T. Matsunaga, J. Biol. Chem. 276:48183–48188, 2001). Here we present a study of the Mms16 protein from *Magnetospirillum gryphiswaldense* to clarify its function. Insertion-duplication mutagenesis of the *mms16* gene did not affect the formation of magnetosome particles but resulted in the loss of the ability of *M. gryphiswaldense* cell extracts to activate poly(3-hydroxybutyrate) (PHB) depolymerization in vitro, which was coincident with loss of the most abundant 16-kDa polypeptide from preparations of PHB granule-bound proteins. The *mms16* mutation could be functionally complemented by enhanced yellow fluorescent protein (EYFP) fused to ApdA, which is a PHB granule-bound protein (phasin) in *Rhodospirillum rubrum* sharing 55% identity to Mms16. Fusions of Mms16 and ApdA to enhanced green fluorescent protein (EGFP) or EYFP were colocalized in vivo with the PHB granules but not with the magnetosome particles after conjugative transfer to *M. gryphiswaldense*. Although the Mms16-EGFP fusion protein became detectable by Western analysis in all cell fractions upon cell disruption, it was predominantly associated with isolated PHB granules. Contrary to previous suggestions, our results argue against an essential role of Mms16 in magnetosome formation, and the previously observed magnetosome localization is likely an artifact due to unspecific adsorption during preparation. Instead, we conclude that Mms16 in vivo is a PHB granule-bound protein (phasin) and acts in vitro as an activator of PHB hydrolysis by *R. rubrum* PHB depolymerase PhaZ1. Accordingly, we suggest renaming the Mms16 protein of *Magnetospirillum* species to ApdA, as in *R. rubrum*.

Magnetotactic bacteria (MTB) form magnetosomes, which are intracellular crystalline magnetic particles that are arranged in chain-like structures (2). In strains of the genus *Magnetospirillum*, magnetosomes consist of magnetite (Fe_3O_4) particles, which are enclosed within intracytoplasmic vesicles formed by the magnetosome membrane (MM) (5). Different phospholipids and a number of specific proteins (MMPs) were found to constitute the MM in various *Magnetospirillum* strains (5–7, 27). In *Magnetospirillum gryphiswaldense*, a comprehensive proteomic analysis of the MM lead to the identification of 18 MMPs, which were present in different amounts. In addition to a number of apparently MTB-specific protein families, proteins with similarity to tetratricopeptide repeat proteins, transporters, and PDZ domain-containing HtrA-like serine proteases were found. Although the individual functions of most of these MMPs have not yet been fully elucidated, they are thought to have functions in the control of redox, pH, iron supersaturation, nucleation, crystal growth, and activation of magnetosome vesicles (5, 17, 37). It is also unknown how these proteins are targeted to the MM during magnetosome assembly and whether the MM originates from the cytoplasmic membrane during the cell cycle.

Although the overall protein profile of magnetosomes from different *Magnetospirillum* strains was markedly different (6), many MMPs are shared between different *Magnetospirillum* strains, and the genetic organization of their genes seems to be highly conserved. For instance, the tetratricopeptide repeat protein MamA was identified in the MM of all three investigated *Magnetospirillum* strains (7, 27, 28). In addition, homologues of the Mms16, Mms6, MamC, and MamD proteins were found associated with isolated magnetosomes in *M. gryphiswaldense* and *Magnetospirillum* sp. strain AMB-1 (1, 6). In *Magnetospirillum* sp. strain AMB-1, Mms16 represented the most abundant magnetosome protein by two-dimensional polyacrylamide gel electrophoresis (27). A putative sequence motif with weak resemblance to a P-Loop (ATP/GTP binding motif) (4, 34) was found (26). Overexpressed Mms16 apparently exhibited GTPase activity in vitro, and the inhibition of cellular GTPases by the addition of AlF_4^- resulted in the impairment or lack of magnetite formation, while the growth of the cells was unaffected in this study. Based on these observations, it was hypothesized by the authors that Mms16 is a magnetosome-associated GTPase, which may be involved in the formation of magnetosomes by triggering the invagination of the

* Corresponding author. Mailing address: Max Planck Institute for Marine Microbiology, Celsiusstr. 1, 28359 Bremen, Germany. Phone: 49 421 2028 746. Fax: 49 421 2028 580. E-mail: dschuele@mpi-bremen.de.

† Present address: Experimental Radiation Oncology, University of Tübingen, Tübingen, Germany.

Downloaded from http://jb.asm.org/ on November 22, 2019 by guest

MM vesicles from the cytoplasmic membrane. The proposed model was in analogy to eukaryotic vesicle budding, which involves priming by small GTPases (3, 43). Because of the presumed association of Mms16 with magnetosomes, this protein was used as a magnetosome-specific anchor molecule to attempt the display of fusion proteins on the surface of magnetosome particles (23, 49).

While Okamura et al. failed to identify homologues of Mms16 in a 2001 database search (26), a number of protein sequences with high similarity to Mms16 were recently identified in the genomes of various nonmagnetic bacteria (6, 11). One of them, ApdA of *Rhodospirillum rubrum*, shares 55% identity with Mms16 of strain AMB-1 (11). The extremely heat- and stress-resistant ApdA protein was recently identified as a poly(3-hydroxybutyrate) (PHB) granule-bound protein (phasin), which is able to stimulate in vitro hydrolysis of native PHB granules isolated from *Wautersia eutropha* by *R. rubrum* PHB depolymerase PhaZ1 (10–12). Evidence was obtained that Mms16 of *M. gryphiswaldense* also may functionally substitute ApdA function (11), since cell extracts of wild-type *M. gryphiswaldense* and of an *Escherichia coli* strain harboring a plasmid with an *mms16-egfp* fusion showed ability to activate PHB granules, comparable to the activity of the native ApdA. In addition, although ApdA activity was detectable both in the soluble and insoluble fractions, it was clearly found to be associated with the PHB granules in vivo, as evident from ApdA-enhanced yellow fluorescent protein (EYFP) fusion experiments with *R. rubrum*. Interestingly, a Mms16-enhanced green fluorescent protein (EGFP) fusion displayed an identical localization pattern if expressed in *R. rubrum* cells. In contrast to Mms16 of *Magnetospirillum* sp. strain AMB-1, no GTPase activity was detectable with purified ApdA of *R. rubrum* (11).

These conflicting observations raised questions about the role of Mms16 in magnetosome biomineralization, as suggested previously (26). On the other hand, both PHB granules and magnetosomes have in common that they are subcellular structures coated by a layer consisting of lipids and a specific subset of proteins. Thus, it might be nevertheless envisioned that Mms16 is a multifunctional protein, which in an unknown way may be involved in the formation of different subcellular structures. Because of the lack of genetic evidence in previous studies and the absence of information about the in vivo localization of the Mms16 protein in magnetospirilla, we aimed to clarify the Mms16 function by the generation of mutants and the analysis of an Mms16-EGFP fusion. *M. gryphiswaldense* was used as a model because this strain can be grown readily and substantial genome sequence data have become available (36). Tools for site-directed mutagenesis have become available for MTB only recently (17, 40). Although a successful procedure was described for *M. gryphiswaldense* (39), the isolation of deletion mutants based on double crossovers can still be a highly tedious task. Therefore, we attempted to establish insertion-duplication mutagenesis as a fast and easy alternative, which is based on gene disruption by a single crossover event resulting in the integration of the used suicide vector into the target gene (8, 20, 25).

MATERIALS AND METHODS

Bacterial strains and plasmids. Strains and plasmids used in this study are listed in Table 1. Strain *M. gryphiswaldense* R3/S1 was referred to as the wild type.

Growth conditions. Cells of *E. coli* were grown at 37°C in Luria-Bertani medium (33). *M. gryphiswaldense* strains were grown microaerobically at 28°C in flask standard medium containing 50 μM ferric citrate as described previously (14). Cultivation on solid medium was performed microaerobically on activated charcoal medium at 28°C (40).

For Mms16 localization and PHB formation studies, recombinant *E. coli* HMS174 harboring pJM9238 (16) with or without *mms16-egfp* was grown in Luria-Bertani medium at 35°C. At an optical density at 600 nm of 1.0, the culture was supplemented with 1% (wt/vol) glucose and the temperature was shifted to 39°C for another 20 h.

DNA techniques. Plasmid isolation and transformation and DNA manipulations in *E. coli* were essentially carried out by standard methods (33). The oligonucleotides used are listed in Table 1.

Biparental mating. Biparental matings were carried out as described previously (40) by using the *E. coli* strain S17-1 as the donor. For homologous recombination, equal amounts (10^9) of cells of *M. gryphiswaldense* R3/S1 and *E. coli* S17-1 were mixed and incubated on plates for 8 h. The cells were flushed from the agar surface and subsequently incubated overnight in sterile liquid medium containing 50 μg of streptomycin/liter. Cells were plated onto activated charcoal medium with rifampin (150 μg/liter) and streptomycin (50 μg/liter) to counterselect against the donor strain and kanamycin (30 μg/liter) to select for the integration of pK19mobsacB suicide plasmids harboring the respective truncated fragments of *mms16*.

Construction of insertion deletion. Several truncated fragments of the *mms16* gene with deletions in the 5′ and 3′ ends were PCR amplified from genomic DNA of *M. gryphiswaldense* with the primers listed in Table 1. The fragments were subcloned into the pGEM-T Easy vector (Promega Mannheim), excised with EcoRI, and ligated into the suicide vector pK19mobsacB. The resulting plasmids pDa97, pDa126, and pDa127 were inserted into the chromosome of *M. gryphiswaldense* R3/S1 by conjugation. This resulted in the mutants Da97 (fragment I, 403 bp), Da126 (fragment II, 309 bp), and Da127 (fragment III, 271 bp). Insertions of plasmids were confirmed by PCR with primers flanking the *mms16* gene (Table 1) and the universal primers M13fw and M13rw that bind within the vector.

Reverse transcription (RT)-PCR. The isolation of the total RNA from *M. gryphiswaldense* was performed by standard techniques (33). Isolated RNA was treated with DNase (MBI Fermentas) and then used in a reverse transcriptase reaction (Moloney murine leukemia virus reverse transcriptase; MBI Fermentas) with primer mmpF1. For a negative control, reverse transcriptase was omitted from the reaction mixture. The obtained cDNA was amplified by using PCR master mix (Promega) and primer pairs *mmpF1* plus *mmpB1* and *mmpF2* plus *mmpB2*, which amplify 309- and 367-bp fragments of the *mms16* gene, respectively.

Complementation of an insertion mutant. For complementation of the *mms16* insertion mutant Da127, the *apdA-eyfp* gene fusion (11) was excised from plasmid pSN2389 by XbaI and SalI digestion and ligated under control of the *lac* promoter into the broad-host-range vector pBBR1MCS5. The resulting plasmid pDa168 was transferred via conjugation into the mutant strain.

Construction of a MamC-EGFP fusion. The *mamC* gene encoding a magnetosome membrane protein of *M. gryphiswaldense* (7) was amplified from genomic DNA with primers *MamCfor* and *MamCSalIrev* containing a SalI site. The PCR product was ligated into the pCR2.1-TOPO vector (Invitrogen), yielding pABC1. The EcoRI-SalI-digested insert from pABC1was then cloned into the corresponding restrictions sites of the pEGFP-N3 vector (BD Clontech) to generate plasmid pABC1. Proper insertion of the in-frame *mamC-egfp* fusion was verified by sequence analysis. The HindIII-XbaI fragment harboring this construct was excised from plasmid pABC1 and subsequently ligated into the HindIII-XbaI sites of pBBR1MCS2 to generate plasmid pABC3. Plasmids used in XbaI digests were previously propagated and isolated from *E. coli* strain INV110 (Invitrogen).

Light and electron microscopy. Light microscopic analysis was performed by using a Zeiss Axioplan fluorescence microscope with phase contrast or fluorescence mode. Zeiss filter no. 15 (for the PHB granules, Nile red staining), 10 (EGFP), and 2 (simultaneous detection of Nile red and EGFP fluorescence) were used. Images were acquired with a digital AxioCam MRc (Zeiss) camera or a CoolsnapCam (Visitron Systems) and processed with the Metaview/Metamorph software (Visitron Systems). For electron microscopy, cells were adsorbed on carbon-coated copper grids. If indicated, they were negatively stained with 2% (wt/vol) uranyl acetate. Samples were viewed and recorded with a JEOL 100CX transmission electron microscope at an accelerating voltage of 100 kV.

Isolation of cell fractions. For the isolation of soluble proteins, membranes, and magnetosomes, French press-disrupted cells were fractionated as described before (6, 7). Native PHB granules were isolated from disrupted cells by two subsequent glycerol density gradient centrifugation as described elsewhere (9).

Downloaded from http://jb.asm.org/ on November 22, 2019 by guest

TABLE 1. Bacterial strains, plasmids, and primers

Strain, plasmid or primer	Description or sequence (5′–3′)	Source or reference
Strains		
E. coli S17-1	*thi pro hsdR recA* with RP4-2[Tc::Mu, Km::Tn*7*]	42
E. coli HMS174	Host for phaCAB	16
R. rubrum		
M. gryphiswaldense R3/S1	Rif^r, Sm^r spontaneous mutant	39
M. gryphiswaldense Da97	Insertion mutant with truncated fragment I of *mms16*	This work
M. gryphiswaldense Da126	Insertion mutant with truncated fragment II of *mms16*	This work
M. gryphiswaldense Da127	Insertion mutant with truncated fragment III of *mms16*	This work
E. coli HMS174	Host for *phaCAB* and/or *phaP*	16
E. coli HMS174(pCS11)	Host for *phaCAB* and pCS11 (*mms16-egfp*)	This work
Plasmids		
pK19mobsacB	Km^r, *sacB* modified from *B. subtilis, lacZ*α	35
pBBR1MCS2	Km^r, *lacZ*α	18
pBBR1MCS5	Gm^r, *lacZ*α	18
pGEM-T Easy	Amp^r, *lacZ*α, PCR cloning vector	Promega
pJM9238	*phaCAB*	16
pSN2389	*apdA-ygfp* fusion in pBBR1MCS2	11
pCS11	*mms16-egfp* fusion in pBBR1MCS2	11
pDa97	pK19mobsacB, containing 403-bp fragment I of *mms16*	This work
pDa126	pK19mobsacB, containing 309-bp fragment II of *mms16*	This work
pDa127	pK19mobsacB, containing 271-bp fragment III of *mms16*	This work
pDa168	pBBR1MCS5 with *apdA-ygfp* fusion	This work
pABC1	*mamC* in pCR-TOPO 2.1 (Invitrogen)	
pABC2	*mamC-egfp* fusion in pEGFP-N3 (Clontech)	
pABC3	*mamC-egfp* fusion in pBBR1MCS2	
Primers		
mmpF1	GGCAGAGCAGCTTTTTGACTTTG	
mmpB1	TTCGCGCATGTTGGACAAC	
mmpB2	CGAACACGTCGCGCATTTC	
mmpF2	TGGACGACCACAAGGTTCCC	
mms16fo6	CATTGCGATGATGGCTGTGC	
mms16rw6	TGCGGAACAAGGTGGATTTG	
M13fw	GTAAAACGACGGCCAGT	
M13rw	CAGGAAACAGCTATGAC	
MamCSallrev	GTCGACGGCCAATTCCCTCA	
MamCfor	TAAGCCTGACCCTTGAAT	

Immunoblot assay. Cells harboring the Mms16-EGFP fusion were fractionated as described above. Forty micrograms of protein of different fractions was separated on sodium dodecyl sulfate (SDS)–16% polyacrylamide gels and blotted onto a polyvinylidene difluoride membrane (Amersham). The membrane was washed for 5 min in Tris-buffered saline (TBS) (pH 7.5), followed by incubation in 6% nonfat dairy milk for 2 h and three washes in TBS–Tween. The blot was incubated for 3 h in a 10^{-2} dilution of the primary antibody (anti-EGFP, no. 8367-1; Clontech) in TBS plus 0.5% bovine serum albumin and rinsed five times in TBS–0.5% bovine serum albumin followed by water for 10 s. Bound antibody was detected by using a 4-Nitro Blue Tetrazolium chloride–5-bromo-4-chloro-3-indolylphosphate staining kit (Roche).

Iron measurement and detection of magnetic orientation. The iron content of the cells was determined by atomic absorption spectroscopy as described previously (7, 14) by using an acytylen air flame (model 3110; Perkin-Elmer, Überlingen, Germany). The average magnetic orientation of cell suspensions was assayed by a light-scattering method as described previously (38).

Determination of ApdA activity. Determinations of the ApdA activities of the cell extracts from different *M. gryphiswaldense* strains were carried out by the measurement of the activity of purified PHB depolymerase PhaZ1 of *R. rubrum* with native PHB (nPHB) isolated from *W. eutropha* H16 in the presence of the cell extracts as described in detail recently (10, 11). Exact quantification of activator activity was not possible, since there is no strict linear correlation between the amount of activator and the velocity and degree of subsequent hydrolysis of nPHB granules. Therefore, experiments were routinely performed at three concentrations of the activator, and the activity was estimated to be present or absent depending on subsequent polymerase reaction. Assays in which the activator was omitted but containing nPHB alone or polymer granules plus PHB depolymerase were routinely performed as controls for autohydrolysis of the granules and activator-independent depolymerase activity, respectively.

Measurement of PHB content. The content of PHB in lyophilized cells was determined by gas chromatography after conversion of PHB into 3-hydroxymethylester by acid-catalyzed methanolysis and with benzoatemethylester as the internal standard.

Analysis of DNA and protein sequence data. Basic analyses of DNA and protein sequences were done by the MacVector, version 7.0, software package (Oxford Molecular Ltd.). Sequence alignments were carried out by using the ClustalW algorithm (45). Protein sequences were compared to the GenBank, EMBL, and SwissProt libraries.

RESULTS

Sequence analysis. The Mms16 proteins of *M. gryphiswaldense* and *Magnetospirillum* sp. strain AMB-1 share 78% identity and 91% similarity. A homologous gene is also present in the unfinished genome assembly of *Magnetospirillum magnetotacticum* strain MS-1 (http://genome.jgi-psf.org/microbial/) with 79% identity to Mms16 of *M. gryphiswaldense* and 91% identity to Mms16 of *Magnetospirillum* sp. strain AMB-1 at the protein level. Analysis of the genomic context of *mms16* did not reveal indications for an operon-like organization in *M. gryphiswaldense*. No further genes with a putative involvement

Downloaded from http://jb.asm.org/ on November 22, 2019 by guest

putative PhbP *A. vinelandii*	42	L	F	E	G	A	E	E	L	A	K	L	Q	F	K	T	I	R	A	A	60
hyp. protein *R. solanacearum*	26	A	F	E	G	V	E	K	L	V	E	L	N	L	Q	V	V	K	A	T	44
gran. assoc. protein *W. eutropha*	26	A	F	E	G	V	E	K	L	V	E	L	N	L	Q	V	V	K	T	T	44
hyp. protein *B. fungorum*	27	A	F	E	G	V	E	K	L	V	E	L	N	L	Q	V	V	K	S	T	45
ApdA *R. rubrum*	48	A	F	E	G	V	Q	A	I	F	K	R	Q	A	E	I	L	R	Q	S	66
Mms16 AMB-1	49	A	F	E	G	L	Q	N	V	V	K	R	Q	V	E	I	L	R	Q	T	67
Mms16 *M. magnetotacticum*	49	A	F	E	G	L	Q	N	V	V	K	R	Q	V	E	I	L	R	Q	T	67
Mms16 *M. gryphiswaldense*	49	A	Y	D	G	L	Q	A	I	F	K	R	Q	A	E	I	L	R	Q	S	67

FIG. 1. Partial sequence alignment of different phasin proteins. The positions of the region are indicated in numbers. Amino acid identities are shown in dark grey, and similarities are shown in light grey. The displayed region represents a putative membrane anchor. hyp., hypothetical; gran. assoc., granule associated.

in magnetosome or PHB metabolism were detected within about 20 kb of sequence flanking *mms16*.

Deduced protein sequences of *mms16* genes predict a hydrophilic 16-kDa protein consisting of 145 amino acids (aa) in all three *Magnetospirillum* strains. The sequence motif characteristic for GTPases (GX_4GK[S/T], where X is any amino acid) (4), which was reported by Okamura et al. (26), was absent or poorly conserved in *Magnetospirillum* sp. strain AMB1 (GSPQGKA or GX_3GKA) and in *M. gryphiswaldense* (GNPQDKA). On the other hand, this motif can also be found in a number of proteins which do not bind ATP or GTP (41). No gene with similarity to *mms16* could be identified in the genome assembly of the magnetotactic coccus MC-1 (http://genome.jgi-psf.org/microbial/). In addition, similarity searches against databases revealed numerous related sequences in nonmagnetotactic bacteria. The closest relative is the PHB granule-bound ApdA (phasin) of *R. rubrum*, which is able to stimulate in vitro hydrolysis of native PHB granules by *R. rubrum* PHB depolymerase PhaZ1 (11, 12) and shares 55% identity and 79% similarity with Mms16 of *M. gryphiswaldense*. Other close hits were found to a number of hypothetical proteins from different bacteria including a hypothetical protein from *Ralstonia metallidurans* (GenBank accession no. ZP_00274201.1; e-value, 8e−22), a hypothetical protein from *Ralstonia eutropha* JMP134Raeut553701 (accession no. ZP_00166578.1; e-value, 3e−18) a hypothetical protein from *Mesorhizobium loti* (accession no. NP_102799.1; e-value, 8e−18), a hypothetical protein from *Burkholderia fungorum* (accession no. ZP_00279851.1; e-value, 1e−10), and a hypothetical protein Bcepa02003463 from *Burkholderia cepacia* (accession no. ZP_00215298.1; e-value, 2e−06). In addition, a number of proteins with weaker similarity were found in BLAST searches, including the PHB granule-associated and hypothetical proteins from the following bacteria of the beta and gamma subdivision: hypothetical protein of *B. fungorum* (accession no. ZP_00035087; e-value, 0.77), PhaP of *Azotobacter* sp. strain FA8 (accession no. CAD42757; e-value, 1.0) (29, 32), putative phasin protein of *Azotobacter vinelandii* (accession no. AAK72594.1; e-value, 1.2), granule-associated protein of *W. eutropha* (accession no. AAC78327; e-value, 3.7), and hypothetical protein from *Ralstonia solanacearum* (accession no. NP_519726; e-value, 8.6) (32). Closer inspection revealed that the similarity to the latter proteins is confined to a short stretch of about 19 amino acids (positions 49 to 67 in Mms16) (Fig. 1), whereas the residual parts of these proteins do not have significant sequence similarity to Mms16.

Mutants with truncated mms16 genes are unaffected in magnetosome biomineralization. Three truncated insertion mutants were generated to clarify the function of Mms16 (Fig. 2). Plasmid insertion resulting from single crossover events occurred with a frequency of about 10^{-6} per recipient cell. After insertion into the chromosome by homologous recombination, the mutants contained two alleles of the *mms16* gene. One copy was truncated in the N terminus by 5 aa in mutants Da97 and Da126, respectively, and by 17 aa in the mutant Da127. This copy is unlikely to be translated due to the absence of a start codon and a ribosomal binding site. In the second copy, 6 aa (Da97) or 38 aa (Da126 and Da127) were deleted from the C terminus. Analysis by RT-PCR confirmed that no full-length transcript of the *mms16* was detectable in mutant strain Da127 (Fig. 2C). Primers mmpF1 and mmpB1 generated a product of 309 bp in the mutant and the wild type as expected. However, primers mmpF2 and mmpB2 failed to amplify a 367-bp fragment in the mutant, confirming the absence of a transcript corresponding to the C terminus.

All three mutants displayed a magnetic reaction as checked by microscopy and light scattering; they accumulated identical amounts of intracellular iron (2.0 to 2.2% iron [dry weight]) and contained chains of magnetosomes, which by electron microscopy were indistinguishable in number, alignment, and shape from those of wild-type cells (Fig. 3).

Truncations in the *mms16* gene affect ApdA activity of mutants. The results of mutagenesis experiments had indicated that magnetosome formation was unaffected by truncations in the *mms16* gene. One explanation for this result may be that the deleted part is not essential for the presumptive function of Mms16 in magnetosome formation. Another possible interpretation is that the metabolic function of Mms16 is entirely different from magnetosome biomineralization. As we previously found that Mms16 could substitute the function of ApdA (12), we analyzed cell extracts obtained from the different mutants for ApdA activity. Extracts from mutant strain Da97 with a truncation of 6 amino acids displayed activity indistinguishable from the *M. gryphiswaldense* wild type. Thus, it can be concluded that these amino acids are irrelevant for ApdA activity. In contrast, cell extracts of the insertion mutants Da126 and Da127 had entirely lost the ApdA activity. The PHB content and number of granules per cell was rather vari-

Downloaded from http://jb.asm.org/ on November 22, 2019 by guest

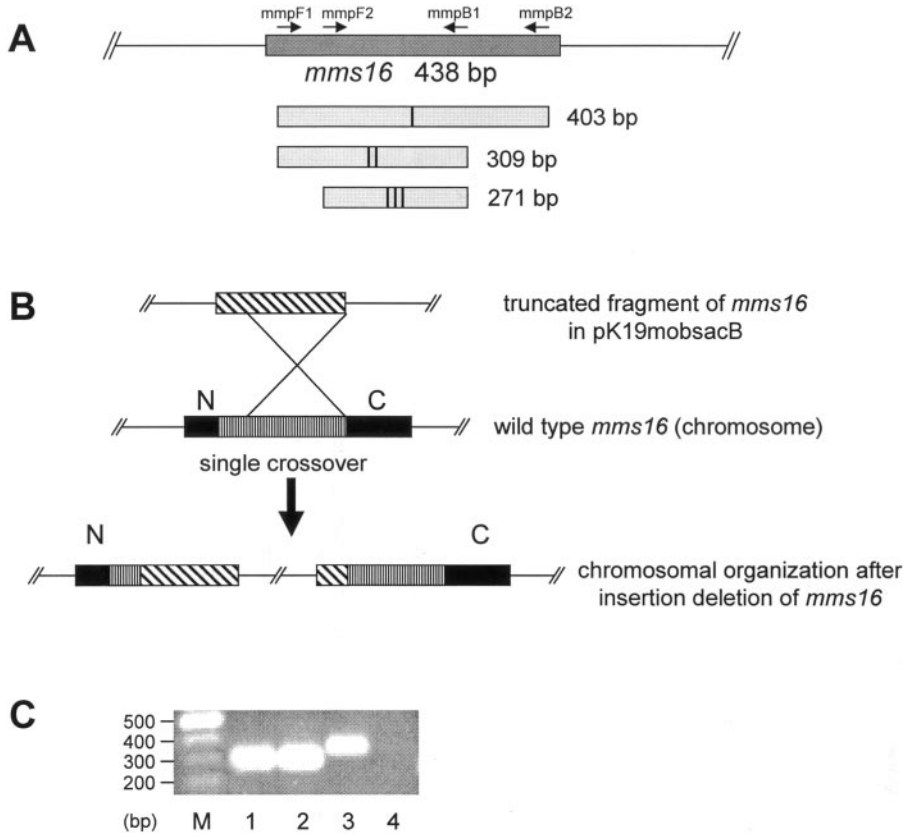

FIG. 2. Schematic representation of the insertion deletion. (A) *mms16* wild-type gene and different truncated fragments (I to III). Sizes are as indicated. (B) Molecular organization of the *mms16* locus before and after insertion-duplication mutagenesis with a truncated fragment. Different fill patterns are used to mark the origins of different parts of the gene after a single crossover. Parts encoding the N and C termini of the corresponding gene products are indicated. (C) Characterization of the Da127 mutant by RT-PCR. The following primer combinations were applied in PCRs: mmpF1 plus mmpB1 (lanes 1 and 2); mmpF1 plus mmpB2 (lanes 3 and 4). A 271-bp truncated fragment was used for mutant construction. Positions of primers are indicated in panel A. cDNA obtained from the wild type (lanes 1 and 3) or the mutant strain Da127 (lanes 2 and 4) was used as a template. Identical reactions with reverse transcriptase omitted were used as negative controls (data not shown).

able between different batches of cells, and we were unable to detect a clear correlation between PHB formation and growth conditions in wild-type and mutant strains. However, the PHB contents of all *M. gryphiswaldense* strains were always in the same range (14 to 24% [dry weight]) as the wild type, which was consistent with electron micrographs and Nile red stains of cells that contained PHB granules comparable in size, number, and appearance (Fig. 3). To ensure that the observed phenotype was caused by deletion of the *mms16* gene and to analyze whether *apdA* and *mms16* are functionally equivalent in vivo, the mutant strain pDa127 was complemented in *trans* with a plasmid harboring a functional copy of *apdA*. Cell extracts of strain Da127 harboring pDa168 with the *apdA-eyfp* fusion (11) showed the same activator activity as the wild type. This result indicates that the disruption of the *mms16* gene can be complemented and that *mms16* can be functionally replaced by ApdA of *R. rubrum*.

Mms16 is localized with PHB granules in vivo and in vitro. While Mms16 was previously found attached to isolated magnetosomes of *M. gryphiswaldense* and *Magnetospirillum* sp. strain AMB-1, an Mms16-EGFP fusion was localized in vivo to the PHB granules in the nonmagnetotactic bacterium *R. rubrum* (11). We found a comparable distribution pattern in recombinant *E. coli* HMS174 expressing *phacab* and the *mms16-egfp* fusion. All visible cellular inclusions showed EGFP- and Nile red-specific fluorescence, confirming the colocalization of Mms16 with PHB. Phasin proteins of other bacteria have been shown to affect the size and number of PHB granules (16, 47). Coexpression of the *mms16-egfp* fusion with the PHB biosynthetic genes of *W. eutropha* in *E. coli* resulted in the formation of an increased number of PHB granules (Fig. 4) comparable to the effect of PhaP of *W. eutropha* or ApdA of *R. rubrum* (11).

To analyze the in vivo localization of Mms16 in its native background, pCS11 harboring an *mms16-egfp* fusion was transferred via conjugation to the *M. gryphiswaldense* wild type and to the nonmagnetic mutant strain MSR-1B (36). In both strains, a punctuate fluorescence pattern over the whole length of the cell was observed (Fig. 5A and C). This pattern was inconsistent with magnetosome localization. For comparison, an EGFP fusion to the magnetosome-associated protein MamC displayed a single fluorescence signal localized in the center of the cell, where the magnetosome chains are usually located (Fig. 5G). Simultaneous staining of the same cell by Nile red revealed that the fluorescence signal from the PHB granules was clearly different from the localization of the

Downloaded from http://jb.asm.org/ on November 22, 2019 by guest

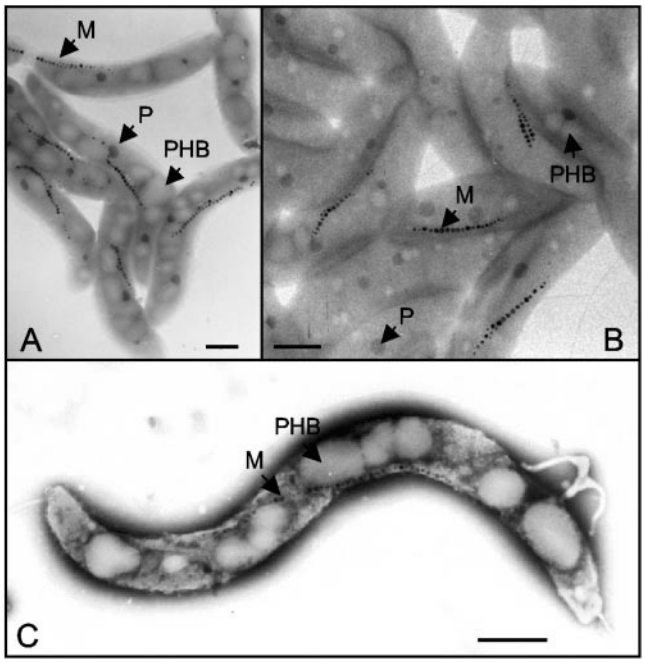

FIG. 3. Electron micrographs of unstained cells of wild-type *M. gryphiswaldense* (A) and strain Da127 (B) and a negatively stained cell of Da127 (C). Arrows indicate PHB granules (*PHB*), magnetosomes (*M*), and polyphosphate globules (*P*). Bars, 0.5 μm.

EGFP fluorescence (Fig. 5E and F). In contrast, simultaneous staining of the cells with Nile red revealed that the fluorescent spots of the *mms16-egfp* fusion coincided with the presence of the PHB granules within the magnetic cells and cells of MSR-1B (Fig. 5A and B). Likewise, the ApdA-EYFP of *R. rubrum* (11) fusion also localized to the PHB granules if pDa168 was conjugated into *M. gryphiswaldense* (Fig. 5D). These results indicate that, identical to the previously observed localization of *mms16-egfp* in *R. rubrum*, the Mms16 protein is also in vivo localized with the PHB granules in *M. gryphiswaldense* but not with the magnetosomes.

The question arose of how this observation relates to the previous identification of the Mms16 protein in isolated magnetosomes (6). We noticed that the presence and intensity of this band was highly variable between different preparations of magnetosomes (data not shown). Magnetosomes isolated from wild-type cells harboring pCS11 exhibited the same protein patterns as magnetosomes from plasmid-free cells, and no additional band that may be expected from the Mms16-EGFP fusion protein (43.3 kDa) was detectable by Coomassie staining (Fig. 6). In contrast, a 16-kDa band was present in SDS extracts of isolated PHB granules, which represented the most abundant protein in this subcellular fraction (we estimate >50% of the total protein) This band, however, was missing in PHB granules isolated from the *mms16* mutant strain Da127. In addition, PHB granules (but not magnetosomes) isolated from the wild-type strain expressing Mms16-EGFP from pCS11 displayed an additional protein band of approximately 43 kDa. In an additional experiment, we used an EGFP-specific antibody in Western blotting to localize the Mms16-EGFP fusion protein in different cell fractions. Figure 7 shows the results of immunostaining of different subcellular fractions obtained from wild-type cells harboring pCS11. In all fractions, the antibody recognized a band of 43 kDa, which is in accordance with the predicted mass of the Mms16-EGFP fusion protein. Taken together, these data indicate that Mms16 in vitro becomes present in detectable but variable amounts in all cell fractions upon cell disruption. However, consistent with its observed in vivo localization, it is predominantly associated with isolated PHB granules.

DISCUSSION

Results obtained in this study indicate that insertion-duplication mutagenesis is an appropriate method for easy and fast deletion of genes within *M. gryphiswaldense*. Although allelic replacement by double crossovers has been recently established in this organism, insertion-duplication mutagenesis offers a great practical advantage as it requires only one cloning step. The frequency of a single crossover event (10^{-6}) is higher by several orders of magnitude than that of double crossovers (10^{-9} to 10^{-10}) (39), and no selection of the second crossover event is required.

In contrast to Okamura et al. (26), who suggested an essential role in magnetosome formation for Mms16 from the closely related *Magnetospirillum* sp. strain AMB-1, our data clearly argue against an involvement of Mms16 in magnetosome biomineralization in *M. gryphiswaldense*. It was speculated by Okamura et al. that Mms16 may function as a small GTPase involved in the formation of intracellular vesicles (26). However, the closely related ApdA of *R. rubrum* failed to hydrolyze GTP in vitro (11), and we were unable to confirm the presence of a conserved GTP- or ATP-binding motif in Mms16 and other analyzed members of this protein family. Okamura et al. (26) further observed that cells grown in the presence of AlF_4^- had interrupted magnetosome chains, and increased concentrations of this inhibitor for GTPases seemed to abolish magnetism, which led them to conclude that GTPase activity is required for magnetite synthesis. However, the interpretation that a particular protein is involved in the observed inhibition is premature, since an inhibition of total cellular GTPases was likely to occur in these experiments. This may have interfered with magnetite formation in a nonspecific manner.

If *mms16* function were fundamental to magnetosome formation, one would expect a universal occurrence of this gene in all magnetotactic bacteria. However, while genes with high similarity to *mms16* are present in *Magnetospirillum* species as well as in a number of nonmagnetotactic bacteria both from the alpha and beta subdivisions of proteobacteria, we were unable to identify a similar gene in the genome of the magnetotactic *Alphaproteobacterium* strain MC-1. For comparison, nearly all others of the identified genes encoding MMPs in *M. gryphiswaldense* have counterparts in the genomes of *M. magnetotacticum* and strain MC-1. Moreover, these *mam* and *mms* genes are clustered within a genomic magnetosome island that is assumed to harbor the genes essential for magnetite biomineralization (36). In *M. gryphiswaldense*, *mms16* is not carried within the magnetosome island nor within an extended genomic region flanking this island (data not shown), which is a further hint that *mms16* may not specifically be related to magnetosome biomineralization.

Downloaded from http://jb.asm.org/ on November 22, 2019 by guest

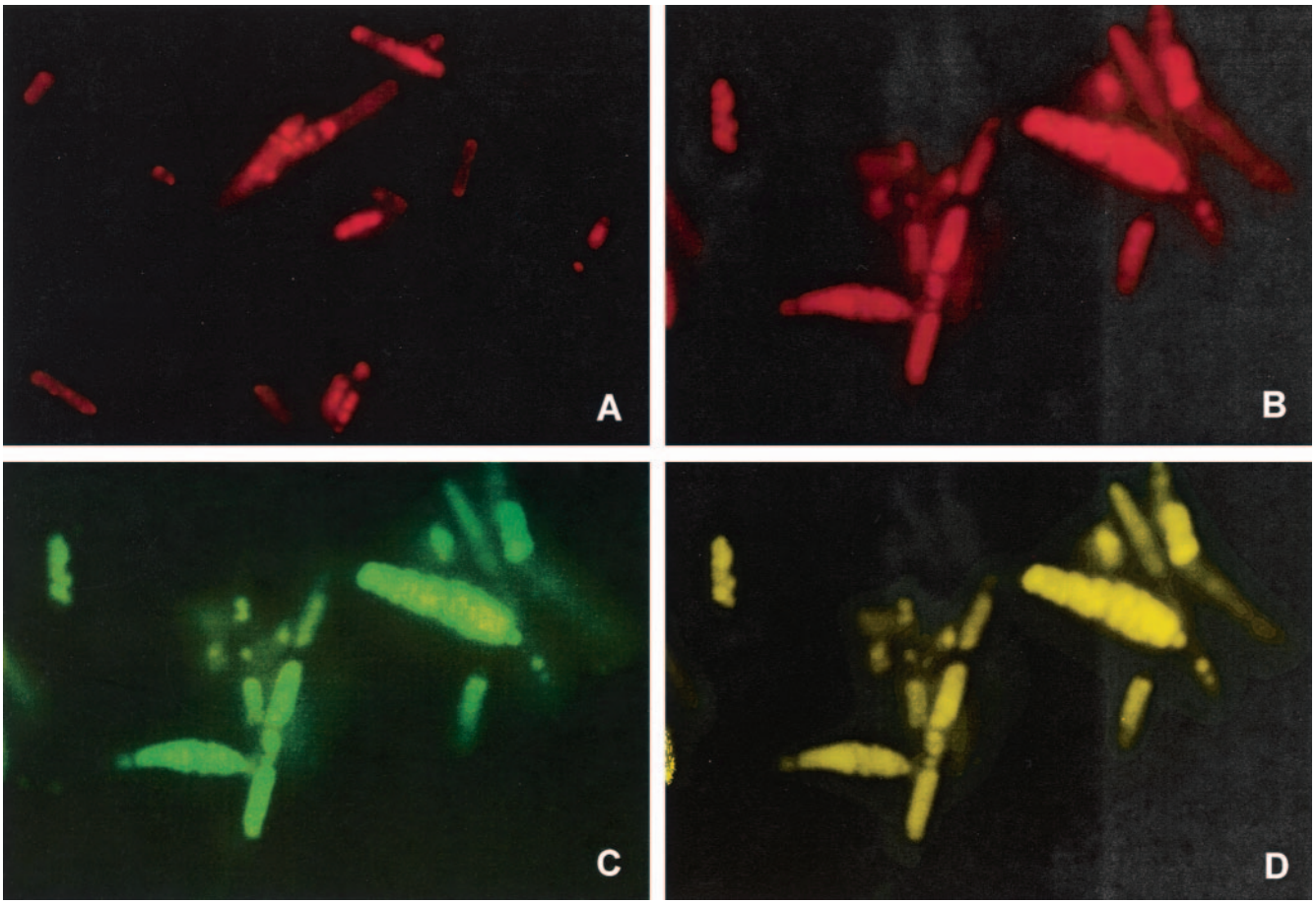

FIG. 4. Fluorescence microscopic analysis of recombinant *E. coli* with *phacab* but without *phaP* (A), and *E. coli* with *phacab* and pCS11 harboring the *mms16-egfp* fusion (B to D). Cells were stained with Nile red and were visualized by using a Nile red (PHB stain)-specific filter (BP546/FT580/LP590) (A, B) or an EGFP-specific filter (BP450-490/FT510/LP515) (C) at 20 h after induction of PHB synthesis. Colocalization of Mms16-EGFP- and Nile red-stained PHB is shown in the fluorescence overlay (D).

Irrespective of its speculated GTPase function, mutagenesis of an abundant magnetosome-associated protein should be expected to have detectable consequences in biomineralization. However, our mutagenesis experiments clearly demonstrated that truncation of a significant part of the protein affected neither the formation of magnetite particles nor their intracellular organization. On the other hand, the mutation abolished the ability of cell extracts from *M. gryphiswaldense* to activate PHB degradation in vitro. Both Mms16 and ApdA in vivo displayed a reciprocal functional equivalence in PHB me-

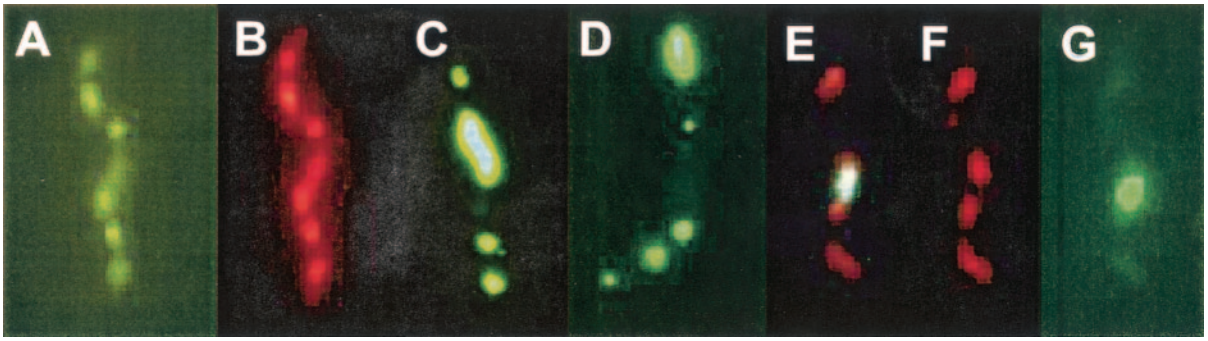

FIG. 5. Localization of various EGFP or EYFP gene fusions in different *M. gryphiswaldense* strains analyzed by fluorescence microscopy. (A) *M. gryphiswaldense* (wild type) plus pCS11 (*mms16-egfp*); (B) Nile red staining of the same cell; (C) nonmagnetic mutant strain MSR-1B plus pCS11; (D) *M. gryphiswaldense* (wild type) plus pDa168 (*apdA-eyfp*). (E to G) *M. gryphiswaldense* (wild type) plus pABC3 stained with Nile red and visualized with the following different filter sets: a Zeiss filter no. 2, visualizing both EGFP and Nile red fluorescence (E), a Nile red-specific filter (F), and an EGFP-specific filter (G).

Downloaded from http://jb.asm.org/ on November 22, 2019 by guest

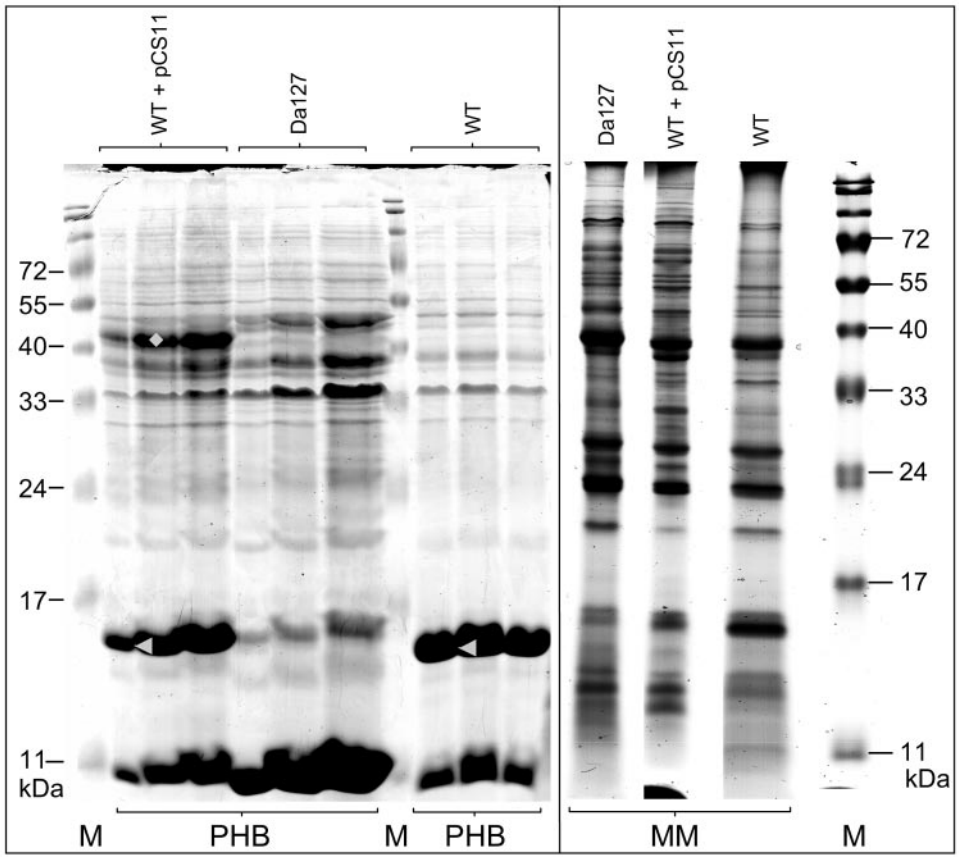

FIG. 6. SDS-polyacrylamide gel electrophoresis of isolated PHB granules (PHB) and isolated magnetosomes (MM) from different *M. gryphiswaldense* strains. Bands presumptively representing the native Mms16 protein are indicated by arrowheads; a band representing the Mms16-EGFP fusion protein is indicated by a diamond. Lane M, molecular mass (in kilodaltons) marker. For better visualization of differences in band intensities, different quantities of PHB proteins (20 to 60 μg per lane) were loaded onto the gel. WT, wild type.

tabolism. This finding is in accordance with the intracellular localization of an Mms16-EGFP, which was localized with PHB granules both in vivo and in vitro. This pattern was indistinguishable from the phasin-like localization of an ApdA-EYFP fusion of *R. rubrum* both in its native background as well as in cells of *M. gryphiswaldense* transformed with pDa168. The localization was independent of the presence of functional magnetosomes, as the nonmagnetic mutant MSR-1B displayed an identical in vivo localization of the Mms16-EGFP fusion. The native Mms16 protein together with the Mms16-EGFP fusion represented the most abundant protein associated with isolated PHB granules. However, despite the rather stringent isolation procedure, Mms16-EGFP was detectable by immunostaining in all subcellular fractions, including isolated magnetosomes. This may be explained by unspecific adsorption of the protein during cell disruption, as cross-contamination by abundant proteins from other subcellular fractions is a common observation that has been reported from the isolation of various complex intracellular structures, such as magnetosomes, PHB granules, and endospores (6, 19, 24, 46).

Because of its PHB-specific localization, Mms16 thus represents a phasin. Phasins are a class of PHB granule-associated proteins. They are characterized by low molecular mass (mostly between 11 and 25 kDa), have an amphiphilic character and high affinity for phytohemagglutinin inclusions, and they mostly contribute a significant fraction to total cell proteins (15, 44, 48). The suggested physiological function of phasins is the stabilization of the hydrophobic granules by preventing coalescence, which is based on the observation that mutants of *W. eutropha* lacking an intact *phaP* (phasin) gene accumulated only a few larger granules compared to the numerous smaller granules present in normal cells (47). *E. coli* expressing the PHB biosynthetic genes except *phaP* produced only a few PHB granules. Apparently, Mms16 has an effect on PHB granule size and number comparable to the effect of PhaP in *R. eutropha* and other PHB-accumulating bacteria and comparable to PhaP or ApdA if these proteins were overexpressed in recombinant *E. coli*.

In contrast, all *mms16* mutants contained PHB granules, which resembled in size and number those found in wild-type cells. One interpretation may be that the function of Mms16 is somewhat different. Another possible explanation may be that additional phasins may compensate for the loss of Mms16. For instance, four phasin genes have been recently identified in the genome sequence of *W. eutropha* (31). Other highly abundant putative phasins, such as a band running slightly above the presumptive Mms16 protein, appeared to be present in preparations of PHB granules (Fig. 6). A further highly abundant

Downloaded from http://jb.asm.org/ on November 22, 2019 by guest

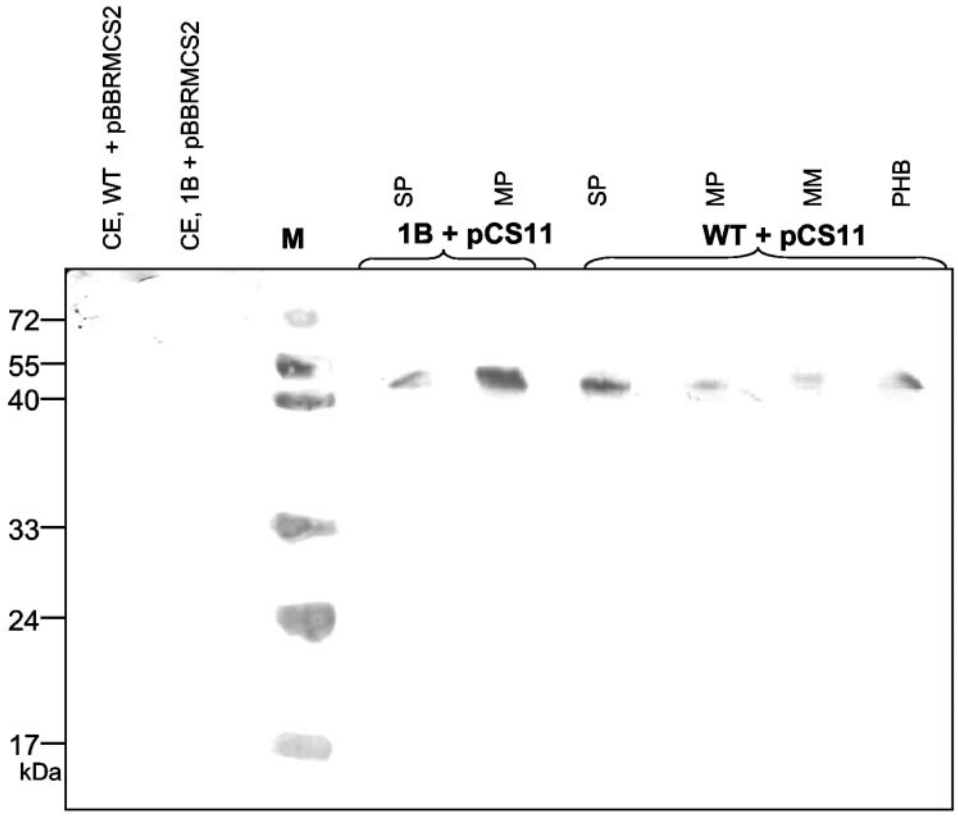

FIG. 7. Western blot analysis of cell fractions from *M. gryphiswaldense* wild type (WT) and the nonmagnetic mutant MSR-1B (1B). The Mms16-EGFP fusion protein was detected by an anti-EGFP antibody. SP, soluble proteins; MP, membrane proteins; MM, magnetosome membrane; PHB, polyhydroxybutyrate; M, molecular mass (in kilodaltons) marker. The left two lanes show crude extracts (CE) of the two strains transformed with pBBRMCS2 that were used as negative controls.

polypeptide was present in the Da127 mutant at approximately 11 kDa, which may either correspond to the truncated Mms16 protein or to a different phasin, whose relative expression seemed to be increased in the mutant compared to the wild type.

Phasins represent a phylogenetically heterogeneous group of proteins (13). With the exception of ApdA homologues, Mms16 displays only low overall sequence similarity to other phasins, and the similarity is confined to a rather hydrophobic stretch of 19 conserved amino acids. Several models for the interactions for phasins with the surface of PHB granules are discussed in the literature. For example, PhaP of *Bacillus megaterium* was described as a hydrophilic protein with no obvious membrane anchor (24). For other granule-associated proteins, two hydrophobic stretches responsible for the anchoring at the carboxyl terminus were described (22, 30). In the *W. eutropha* phasin, four hydrophobic domains were suggested as putative anchors (13, 21, 24). Since the overall sequences of Mms16 and ApdA predict highly hydrophilic proteins, it can be speculated that the identified 19-aa motif in Mms16 is anchoring the protein to the surface of PHB granules. Such an anchor may also be responsible for the observed tendency of Mms16 to attach to other cellular fractions during cell disruption.

In summary, these different lines of evidence show that Mms16 is not a native magnetosome protein and has no obvious role in magnetite biomineralization in *M. gryphiswaldense*. Instead, it must be concluded that its function is homologous to that of the highly similar ApdA protein, which is bound to PHB granules in *R. rubrum* (11, 12). We therefore propose the renaming of Mms16 to ApdA, as in *R. rubrum*. Given the high genetic similarity between *M. gryphiswaldense* and strain AMB-1, its role in magnetosome formation as previously suggested (26) seems questionable and will also require clarification in the latter organism. This is of particular importance, as subsequent studies have proposed the use of Mms16 as an anchor molecule to display fusion proteins specifically on the surface of magnetosomes (23, 49), which will require reassessment in future studies.

ACKNOWLEDGMENTS

This study was supported by the BMBF BioFuture program, the Max Planck Society, and the Deutsche Forschungsgemeinschaft.

We thank Katja Schmidt for excellent technical assistance and Karen Grünberg and Astrid Bartel for help with plasmid construction.

REFERENCES

1. **Arakaki, A., J. Webb, and T. Matsunaga.** 2003. A novel protein tightly bound to bacterial magnetic particles in *Magnetospirillum magneticum* strain AMB-1. J. Biol. Chem. **278:**8745–8750.
2. **Bazylinski, D. A., and R. B. Frankel.** 2004. Magnetosome formation in prokaryotes. Nat. Rev. Microbiol. **2:**217–230.
3. **Bonifacino, J. S., and B. S. Glick.** 2004. The mechanisms of vesicle budding and fusion. Cell **116:**153–166.
4. **Bourne, H. R., D. A. Sanders, and F. McCormick.** 1991. The GTPase superfamily: conserved structure and molecular mechanism. Nature **349:**117–127.

Downloaded from http://jb.asm.org/ on November 22, 2019 by guest

5. **Gorby, Y. A., T. J. Beveridge, and R. P. Blakemore.** 1988. Characterization of the bacterial magnetosome membrane. J. Bacteriol. **170:**834–841.
6. **Grünberg, K., E. C. Muller, A. Otto, R. Reszka, D. Linder, M. Kube, R. Reinhardt, and D. Schüler.** 2004. Biochemical and proteomic analysis of the magnetosome membrane in *Magnetospirillum gryphiswaldense*. Appl. Environ. Microbiol. **70:**1040–1050.
7. **Grünberg, K., C. Wawer, B. M. Tebo, and D. Schüler.** 2001. A large gene cluster encoding several magnetosome proteins is conserved in different species of magnetotactic bacteria. Appl. Environ. Microbiol. **67:**4573–4582.
8. **Hamilton, H. L., K. J. Schwartz, and J. P. Dillard.** 2001. Insertion-duplication mutagenesis of *Neisseria*: use in characterization of DNA transfer genes in the gonococcal genetic island. J. Bacteriol. **183:**4718–4726.
9. **Handrick, R., S. Reinhardt, M. L. Focarete, M. Scandola, G. Adamus, M. Kowalczuk, and D. Jendrossek.** 2001. A new type of thermoalkalophilic hydrolase of *Paucimonas lemoignei* with high specificity for amorphous polyesters of short chain-length hydroxyalkanoic acids. J. Biol. Chem. **276:**36215–36224.
10. **Handrick, R., S. Reinhardt, P. Kimmig, and D. Jendrossek.** 2004. The "intracellular" PHB depolymerase of *Rhodospirillum rubrum* is a periplasm-located protein with specificity for native PHB and with structural similarity to extracellular PHB depolymerases. J. Bacteriol. **186:**7243–7253.
11. **Handrick, R., S. Reinhardt, D. Schultheiss, T. Reichart, D. Schüler, V. Jendrossek, and D. Jendrossek.** 2004. Unraveling the function of the *Rhodospirillum rubrum* activator of polyhydroxybutyrate (PHB) degradation: the activator is a PHB-granule-bound protein (phasin). J. Bacteriol. **186:**2466–2475.
12. **Handrick, R., U. Technow, T. Reichart, S. Reinhardt, T. Sander, and D. Jendrossek.** 2004. The activator of the *Rhodospirillum rubrum* PHB depolymerase is a polypeptide that is extremely resistant to high temperature (121 degrees C) and other physical or chemical stresses. FEMS Microbiol. Lett. **230:**265–274.
13. **Hanley, S. Z., D. J. Pappin, D. Rahman, A. J. White, K. M. Elborough, and A. R. Slabas.** 1999. Re-evaluation of the primary structure of *Ralstonia eutropha* phasin and implications for polyhydroxyalkanoic acid granule binding. FEBS Lett. **447:**99–105.
14. **Heyen, U., and D. Schüler.** 2003. Growth and magnetosome formation by microaerophilic *Magnetospirillum* strains in an oxygen-controlled fermentor. Appl. Microbiol. Biotechnol. **61:**536–544.
15. **Jurasek, L., and R. H. Marchessault.** 2002. The role of phasins in the morphogenesis of poly(3-hydroxybutyrate) granules. Biomacromolecules **3:**256–261.
16. **Kidwell, J., H. E. Valentin, and D. Dennis.** 1995. Regulated expression of the *Alcaligenes eutrophus pha* biosynthesis genes in *Escherichia coli*. Appl. Environ. Microbiol. **61:**1391–1398.
17. **Komeili, A., H. Vali, T. J. Beveridge, and D. K. Newman.** 2004. Magnetosome vesicles are present before magnetite formation, and MamA is required for their activation. Proc. Natl. Acad. Sci. USA **101:**3839–3844.
18. **Kovach, M. E., P. H. Elzer, D. S. Hill, G. T. Robertson, M. A. Farris, R. M. Roop II, and K. M. Peterson.** 1995. Four new derivatives of the broad-host-range cloning vector pBBR1MCS, carrying different antibiotic-resistance cassettes. Gene **166:**175–176.
19. **Lai, E. M., N. D. Phadke, M. T. Kachman, R. Giorno, S. Vazquez, J. A. Vazquez, J. R. Maddock, and A. Driks.** 2003. Proteomic analysis of the spore coats of *Bacillus subtilis* and *Bacillus anthracis*. J. Bacteriol. **185:**1443–1454.
20. **Lee, M. S., C. Seok, and D. A. Morrison.** 1998. Insertion-duplication mutagenesis in *Streptococcus pneumoniae*: targeting fragment length is a critical parameter in use as a random insertion tool. Appl. Environ. Microbiol. **64:**4796–4802.
21. **Liebergesell, M., B. Schmidt, and A. Steinbüchel.** 1992. Isolation and identification of granule-associated proteins relevant for poly(3-hydroxyalkanoic acid) biosynthesis in *Chromatium vinosum* D. FEMS Microbiol. Lett. **78:**227–232.
22. **Madison, L. L., and G. W. Huisman.** 1999. Metabolic engineering of poly(3-hydroxyalkanoates): from DNA to plastic. Microbiol. Mol. Biol. Rev. **63:**21–53.
23. **Matsunaga, T., H. Takeyama, and Y. Okamura.** 11 March 2004. Magnetic particle membrane-specific protein. U. S. patent application 10/450,346.
24. **McCool, G. J., and M. C. Cannon.** 1999. Polyhydroxyalkanoate inclusion body-associated proteins and coding region in *Bacillus megaterium*. J. Bacteriol. **181:**585–592.
25. **Morrison, D. A., M. C. Trombe, M. K. Hayden, G. A. Waszak, and J. D. Chen.** 1984. Isolation of transformation-deficient *Streptococcus pneumoniae* mutants defective in control of competence, using insertion-duplication mutagenesis with the erythromycin resistance determinant of pAMβ1. J. Bacteriol. **159:**870–876.
26. **Okamura, Y., H. Takeyama, and T. Matsunaga.** 2001. A magnetosome-specific GTPase from the magnetic bacterium *Magnetospirillum magneticum* AMB-1. J. Biol. Chem. **276:**48183–48188.
27. **Okamura, Y., H. Takeyama, and T. Matsunaga.** 2000. Two-dimensional analysis of proteins specific to the bacterial magnetic particle membrane from *Magnetospirillum* sp. AMB-1. Appl. Biochem. Biotechnol. **84–86:**441–446.
28. **Okuda, Y., K. Denda, and Y. Fukumori.** 1996. Cloning and sequencing of a gene encoding a new member of the tetratricopeptide protein family from magnetosomes of *Magnetospirillum magnetotacticum*. Gene **171:**99–102.
29. **Pettinari, J. M., L. Chaneton, G. Vazquez, A. Steinbüchel, and B. S. Mendez.** 2003. Insertion sequence-like elements associated with putative polyhydroxybutyrate regulatory genes in *Azotobacter* sp. FA8. Plasmid **50:**36–44.
30. **Pieper-Fürst, U., M. H. Madkour, F. Mayer, and A. Steinbüchel.** 1995. Identification of the region of a 14-kilodalton protein of *Rhodococcus ruber* that is responsible for the binding of this phasin to polyhydroxyalkanoic acid granules. J. Bacteriol. **177:**2513–2523.
31. **Pötter, M., H. Müller, F. Reinecke, R. Wieczorek, F. Fricke, B. Bowien, B. Friedrich, and A. Steinbüchel.** 2004. The complex structure of polyhydroxybutyrate (PHB) granules: four orthologous and paralogous phasins occur in *Ralstonia eutropha*. Microbiology **150:**2301–2311.
32. **Salanoubat, M., S. Genin, F. Artiguenave, J. Gouzy, S. Mangenot, M. Arlat, A. Billault, P. Brottier, J. C. Camus, L. Cattolico, M. Chandler, N. Choisne, C. Claudel-Renard, S. Cunnac, N. Demange, C. Gaspin, M. Lavie, A. Moisan, C. Robert, W. Saurin, T. Schiex, P. Siguier, P. Thebault, M. Whalen, P. Wincker, M. Levy, J. Weissenbach, and C. A. Boucher.** 2002. Genome sequence of the plant pathogen *Ralstonia solanacearum*. Nature **415:**497–502.
33. **Sambrook, J., and D. W. Russel.** 2001. Molecular cloning: a laboratory manual, 3rd ed. Cold Spring Harbor Laboratory Press, Cold Spring Harbor, N.Y.
34. **Saraste, M., P. R. Sibbald, and A. Wittinghofer.** 1990. The P-loop—a common motif in ATP- and GTP-binding proteins. Trends Biochem. Sci. **15:**430–434.
35. **Schäfer, A., A. Tauch, W. Jager, J. Kalinowski, G. Thierbach, and A. Pühler.** 1994. Small mobilizable multi-purpose cloning vectors derived from the *Escherichia coli* plasmids pK18 and pK19: selection of defined deletions in the chromosome of *Corynebacterium glutamicum*. Gene **145:**69–73.
36. **Schübbe, S., M. Kube, A. Scheffel, C. Wawer, U. Heyen, A. Meyerdierks, M. H. Madkour, F. Mayer, R. Reinhardt, and D. Schüler.** 2003. Characterization of a spontaneous nonmagnetic mutant of *Magnetospirillum gryphiswaldense* reveals a large deletion comprising a putative magnetosome island. J. Bacteriol. **185:**5779–5790.
37. **Schüler, D.** 2004. Molecular analysis of a subcellular compartment: the magnetosome membrane in *Magnetospirillum gryphiswaldense*. Arch. Microbiol. **181:**1–7.
38. **Schüler, D., R. Uhl, and E. Baeuerlein.** 1995. A simple light-scattering method to assay magnetism in *Magnetospirillum gryphiswaldense*. FEMS Microbiol. Lett. **132:**139–145.
39. **Schultheiss, D., M. Kube, and D. Schüler.** 2004. Inactivation of the flagellin gene *flaA* in *Magnetospirillum gryphiswaldense* results in nonmagnetotactic mutants lacking flagellar filaments. Appl. Environ. Microbiol. **70:**3624–3631.
40. **Schultheiss, D., and D. Schüler.** 2003. Development of a genetic system for *Magnetospirillum gryphiswaldense*. Arch. Microbiol. **179:**89–94. (First published 15 Nov 2002; 10.1007/s00203-002-0498-z.)
41. **Sigrist, C. J., L. Cerutti, N. Hulo, A. Gattiker, L. Falquet, M. Pagni, A. Bairoch, and P. Bucher.** 2002. PROSITE: a documented database using patterns and profiles as motif descriptors. Brief. Bioinform. **3:**265–274.
42. **Simon, R., U. Priefer, and A. Pühler.** 1983. A broad host range mobilisation system for *in vivo* genetic engineering: transposon mutagenesis in Gram-negative bacteria. Bio/Technology **1:**784–791.
43. **Springer, S., A. Spang, and R. Schekman.** 1999. A primer on vesicle budding. Cell **97:**145–148.
44. **Steinbüchel, A., K. Aerts, W. Babel, C. Follner, M. Liebergesell, M. H. Madkour, F. Mayer, U. Pieper-Fürst, A. Pries, H. E. Valentin, et al.** 1995. Considerations on the structure and biochemistry of bacterial polyhydroxyalkanoic acid inclusions. Can. J. Microbiol. **41**:94–105.
45. **Thompson, J. D., D. G. Higgins, and T. J. Gibson.** 1994. CLUSTAL W: improving the sensitivity of progressive multiple sequence alignment through sequence weighting, position-specific gap penalties and weight matrix choice. Nucleic Acids Res. **22:**4673–4680.
46. **Todd, S. J., A. J. Moir, M. J. Johnson, and A. Moir.** 2003. Genes of *Bacillus cereus* and *Bacillus anthracis* encoding proteins of the exosporium. J. Bacteriol. **185:**3373–3378.
47. **Wieczorek, R., A. Pries, A. Steinbüchel, and F. Mayer.** 1995. Analysis of a 24-kilodalton protein associated with the polyhydroxyalkanoic acid granules in *Alcaligenes eutrophus*. J. Bacteriol. **177:**2425–2435.
48. **York, G. M., J. Stubbe, and A. J. Sinskey.** 2001. New insight into the role of the PhaP phasin of *Ralstonia eutropha* in promoting synthesis of polyhydroxybutyrate. J. Bacteriol. **183:**2394–2397.
49. **Yoshino, T., M. Takahashi, H. Takeyama, Y. Okamura, F. Kato, and T. Matsunaga.** 2004. Assembly of G protein-coupled receptors onto nanosized bacterial magnetic particles using Mms16 as an anchor molecule. Appl. Environ. Microbiol. **70:**2880–2885.

Downloaded from http://jb.asm.org/ on November 22, 2019 by guest